Journal of Hydrology 568 (2019) 611–625

Contents lists available at ScienceDirect

Journal of Hydrology

journal homepage: www.elsevier.com/locate/jhydrol

Review papers

Complex influences of meteorological drought time-scales on hydrological droughts in natural basins of the contiguous Unites States

Marina Peña-Gallardo[a,*], Sergio M. Vicente-Serrano[a], Jamie Hannaford[b,h], Jorge Lorenzo-Lacruz[c], Mark Svoboda[d], Fernando Domínguez-Castro[a], Marco Maneta[e], Miquel Tomas-Burguera[f], Ahmed El Kenawy[a,g]

[a] Instituto Pirenaico de Ecología, Consejo Superior de Investigaciones Científicas (IPE–CSIC), Spain
[b] Centre for Ecology and Hydrology, UK
[c] University of the Balearic Islands, Spain
[d] National Drought Mitigation Centre, University of Nebraska-Lincoln, United States
[e] Geosciences Department, University of Montana, Missoula, United States
[f] Estación Experimental de Aula Dei, Consejo Superior de Investigaciones Científicas (EEAD-CSIC), Spain
[g] Department of Geography, Mansoura University, Mansoura, Egypt
[h] Irish Climate Analysis and Research UnitS (ICARUS) Maynooth University, Ireland.

ARTICLE INFO

This manuscript was handled by Marco Borga, Editor-in-Chief, with the assistance of Yuting Yang, Associate Editor

Keywords:
Hydrological drought
Climatic drought
Time-scales
Drought propagation
SPEI
Natural basins
Climate variability

ABSTRACT

We analyzed the relationships between meteorological drought and hydrological drought using very dense and diverse network of gauged natural drainage basins across the conterminous U.S. Specifically, this work utilized a dataset of 289 gauging stations, covering the period 1940–2013. Drainage basins were obtained for each gauging station using a digital terrain model. In addition to meteorological data (e.g., precipitation, air temperature and the atmospheric evaporative demand), we obtained a number of topographic, soil and remote sensing variables for each defined drainage basin. A hydrological drought index (the Standardized Streamflow Index; SSI) was computed for each basin and linked to the Standardized Precipitation Evapotranspiration Index (SPEI), which was used as a metric of climatic drought severity. The relationships between different SPEI time-scales and their corresponding SSI were assessed by means of a Pearson correlation coefficient. Also, the general patterns of response of hydrological droughts to climatic droughts were identified using a principal component analysis. Overall, results demonstrate a positive response of SSI to SPEI at shorter time-scales, with strong seasonality and clear spatial differences. We also assessed the role of some climatic and environmental factors in explaining these different responses using a predictive discriminant analysis. Results indicate that elevation and vegetation coverage are the main drivers of the diverse response of SSI to SPEI time-scales. Similar analyses were made for three sub-periods (1940–1964, 1965–1989 and 1989–2013), whose results confirm considerable differences in the response of SSI to SPEI over the past eighty years.

1. Introduction

Hydrological drought has the potential for having severe economic, social and environmental consequences (Van Loon, 2015), being a complex phenomenon that is yet not fully understood (Tallaksen and Van Lanen, 2004). While there is an evident connection between hydrological droughts and climatic variability, other human and environmental factors may impact the duration, extent, and severity of hydrological droughts along with their associated damage (Lorenzo-Lacruz et al., 2013; Bąk and Kubiak-Wójcicka, 2017; Tijdeman et al., 2018). Furthermore, correctly attributing the causes of hydrological droughts remains a challenge given the varying and complex relationship between climate moisture deficits and water deficits in different systems, which is a consequence of the complex character of drought propagation throughout the hydrological cycle, particularly in drainage basins with diverse physical characteristics and management practices (Tallaksen et al., 2004; Sheffield and Wood, 2011; Van Loon, 2015).

McKee et al. (1993) developed the concept of drought time-scale to characterize the system response period from the arrival of water inputs to the time water is available for different usable resources (e.g., soil moisture, groundwater, snowpack, streamflow, lake levels and reservoir storages). Indeed, the response time to a climatic drought condition

* Corresponding author.
E-mail address: marinapgallardo@ipe.csic.es (M. Peña-Gallardo).

https://doi.org/10.1016/j.jhydrol.2018.11.026
Received 10 July 2018; Received in revised form 28 September 2018; Accepted 7 November 2018
Available online 17 November 2018

varies significantly between these different usable water sources. For example, soil moisture usually responds at short climate drought time-scales (Scaini et al., 2015), while reservoir storages and groundwater levels respond to drought at longer time-scales (Bloomfield et al., 2015; Lorenzo-Lacruz et al., 2010 and 2017). Streamflows show a complex response that is dependent on a variety of natural and anthropogenic factors, including –among others- climatic and topographic characteristics, land cover and use, and management practices (López-Moreno et al., 2013; Lorenzo-Lacruz et al., 2013; Barker et al., 2016). Recent studies show that the response of streamflows to climatic droughts of different time scales is complex and multifaceted (Merheb et al., 2016; Huang et al., 2017; Wu et al., 2017; Tijdeman et al., 2018).

Although some studies have argued that anthropogenic factors (e.g., water management practices, water regulation and use) are the most important in determining the response of streamflow droughts to different climatic drought time-scales (López-Moreno et al., 2009; Lorenzo-Lacruz et al., 2013; Wu et al., 2017), the physical characteristics of a basin area are also very important factors and contribute critical information to explaining the different response of streamflow droughts to climatic drought time-scales. For example, Vicente-Serrano et al. (2011) analyzed the response of two relatively undisturbed upstream watersheds located in northeastern Spain, and found they presented a complex and contrasting response to climatic drought time-scales. In particular, while one of these two watersheds responded to short (< 3 months) climatic drought time-scales, the other responded to a very long (> 40 months) time-scales. This contrasting response was mainly attributed to the differing dominant lithology of each basin. Similarly, Barker et al. (2016) analyzed the relationship between hydrological and climatic droughts in different natural catchments in the UK. They reported strong differences in the response of hydrological droughts to climatic droughts linked to the different lithology and aquifer characteristics of the catchments.

For instance physiographic variables (e.g., area, topography, slope, etc.), and vegetation coverage are important controls mediating the effect of climatological drought on streamflows, as confirmed by many studies worldwide. One representative example is Van Loon and Laaha (2015), who concluded that streamflow drought duration in Austria is controlled primarily by catchment properties that define storage and release dynamics (e.g. geology and land use). What these studies show is that biophysical factors control not only streamflow drought characteristics (e.g. duration and severity), but also the sensitivity of streamflow drought to climatic drought at different time-scales. However, disentangling the role of individual factors and attributing their contribution to the response of hydrological drought to climatic drought conditions is an unresolved problem, which is complicated by anthropogenic modifications as well as by the intrinsic non-linear dynamics of hydrologic systems.

In the United States, Abatzoglou et al. (2014) used a range of drought indices to analyze streamflow anomalies in the U.S. Pacific Northwest and the stationarity of the relationship between climatic and streamflow dynamics, while Tijdeman et al. (2016) analyzed streamflow drought duration in > 800 catchments across the US. They found that drought duration characteristics vary among the different climate regimes, with precipitation playing the main role in these spatial variations. However, these studies did not analyze the role that catchment characteristics play on the propagation of climatic drought to streamflows.

In this study we fill a gap in our understanding of how climatic droughts propagate through the hydrologic system. The objectives of this study are fourfold: (i) to determine the climatic drought time-scales that better explain the hydrologic drought as reflected in streamflow anomalies over a wide range of natural basins across the conterminous United States (CONUS), (ii) to identify and analyze spatial patterns and gradients in the climatic-hydrologic drought response, (iii) to explore the role that different environmental factors play in shaping the sensitivity of streamflows to climatic drought, and (iv) to identify possible non-stationarities in the climate-streamflow relationship. This study employs long-term monthly streamflow records from the USGS Hydro-Climatic Data Network, which covers all hydroclimatic regions in the CONUS and provides a solid base from which we can gain insight into how streamflow responds to climatic drought.

2. Data and methods

2.1. Datasets

2.1.1. Streamflow time series

Streamflow time series for our analysis were obtained from the USGS Hydro-Climatic Data Network 2009 (HCDN-2009), which includes monthly streamflow records from 702 hydrological gauges located in catchments with low anthropogenic perturbations. Further details about the characteristics of this dataset (e.g. data quality, data completeness, spatial and temporal coverage, etc.) can be obtained at (http://water.usgs.gov/osw/hcdn-2009/). From the 702 gauges included in the HCDN-2009, we restricted our analysis to those gauges covering the period 1940–2013 and with less than 15% missing data. Following these criteria, we selected 289 stations, whose spatial distribution is illustrated in Fig. 1. The selected gauges cover the entire CONUS, although sampling densities are higher along the eastern and western coasts, the Inter-mountain West and the Midwest regions of the country. Gaps in the streamflow time series were completed using data from a standardized composite reference series built from the most correlated series with the target series, and using percentiles with the purpose of maintaining the temporal variance of the series.

2.1.2. Climatic information

Monthly gridded precipitation and temperature data were obtained from the PRISM (Parameter-elevation Relationships on Independent Slopes Model) product developed by Oregon State University (http://www.prism.oregonstate.edu/, \Daly et al., 2008). PRISM has been widely used for climatic, hydrological, agricultural and environmental applications in the U.S. (e.g. Lutz et al., 2010; Bandaru et al., 2017; Bodner and Robles, 2017). In this study, we employed monthly precipitation, maximum and minimum air temperatures from 1940 to 2013, provided by PRISM at 30 s (approximately 10 km) resolution. Monthly Reference Evapotranspiration (ETo) was calculated from using the Hargreaves method (Hargreaves and Samani, 1985). The Hargreaves-Samani method is recommended under data scarcity conditions (Allen, 1998), as it estimates ETo using only maximum and minimum air temperatures and the extraterrestrial solar radiation calculated using the latitude and the Julian day. Finally, precipitation and ETo grids were used to calculate the climatic balance, defined as the difference between precipitation and ETo.

2.1.3. Physiography and land cover

Elevation data for the CONUS was obtained from the USGS Digital Elevation Model (DEM) (https://lta.cr.usgs.gov/GMTED2010). Vegetation characteristics were assessed using the Normalized Difference Vegetation Index (NDVI) dataset derived from reflectance bands obtained by the Advanced Very high Resolution Radiometer (AVHRR) sensor (https://www.star.nesdis.noaa.gov/smcd/emb/vci/VH/vh_browse.php) at a spatial resolution of 1.1 km. The NDVI is a reflectance-based variable, closely related to the vegetation coverage, biomass and leaf area index (Carlson and Ripley, 1997).

Relevant high-resolution soil variables (e.g., depth of soil layer, soil drainage, water field capacity, infiltration capacity and soil permeability) were obtained from the USDA's State Soil Geographic (STATSGO, 1991) database (USDA, 1991). Data of all variables were derived for each individual basin incorporating some of the selected streamflow gauges. The boundaries of each drainage basin were defined using the DEM data within the ArcGIS platform. Average monthly and seasonal climate data were obtained for each basin independently.

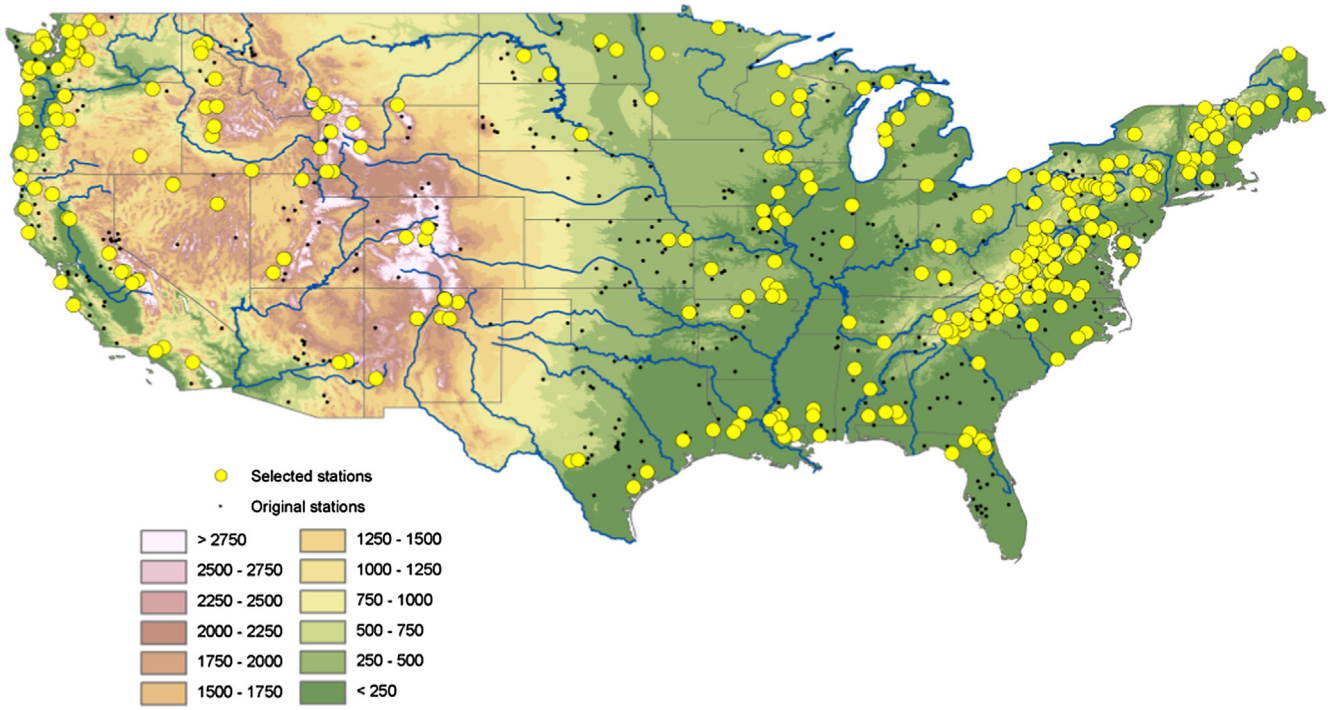

Fig. 1. Spatial distribution of the available (black dots) and the selected (yellow circles) near-natural streamflow gauges across the U.S. Elevation is given in meters. (For interpretation of the references to colour in this figure legend, the reader is referred to the web version of this article.)

Seasons were defined as: cold season (ONDJFM) and warm season (AMJJAS).

2.2. Methods

2.2.1. Hydrological drought definition

We used the Standardized Streamflow Index (SSI) to quantify streamflow drought severity (Vicente-Serrano et al., 2012). Since the SSI is a standardized quantity, it permits direct comparison between gauges, and between different time periods, irrespective of the magnitude and seasonality of streamflow series. The SSI transforms monthly streamflow time series into a time series of probabilities by first calculating a dimensionless time series of standardized streamflow anomalies using different distribution fits for each month/station. We used a wide range of candidate probability distributions, including the general extreme value, the Pearson Type III (PIII), the log-logistic, the log-normal, the generalized Pareto and the Weibull distributions. The selection based on the minimum orthogonal distance between the L-moments of the sampled dataset and the L-moment of a candidate continuous distribution.

More details on the SSI calculation can be found in Vicente-Serrano et al. (2012).

2.2.2. Climatic drought indices

There is a large amount of drought indices based on climate information (Heim, 2002), existing recent developments like the Evaporative Demand Drought Index (EDDI) (Hobbins et al., 2016) or the Standardized Evapotranspiration Deficit Index (SEDI) (Vicente-Serrano et al., 2018). Here, to characterize climatic anomalies, we used two of the most common climatic drought indices, the Standardization Precipitation Index (SPI) and the Standardization Precipitation Evapotranspiration Index (SPEI). The SPI was proposed by McKee et al. (1993) and has been widely used during the last two decades due to its solid theoretical development, robustness, and versatility in drought analyses (Redmond, 2002). As such, it has been recommended by the World Meteorological Organization as the reference index for meteorological drought (WMO, 2012). Like the SSI, the SPI is based on the conversion of precipitation anomalies to probabilities using long-term records. The anomalies are accumulated over periods of a specified length, which produce a time series of anomalies representing a characteristic time-scale. The main advantage of the SPI is that it allows for analyzing drought impacts at different temporal scales, which can then be compared to anomalies from datasets representing other drought types (i.e. meteorological, hydrological and economic). The SPI has been widely used for this purpose in several studies (e.g. Vicente-Serrano and López-Moreno 2005; Fiorillo and Guadagno 2010; Lorenzo-Lacruz et al., 2010; Vicente-Serrano et al., 2011).

The main criticism of the SPI is that its calculation is based solely on precipitation data and does not account for other meteorological factors (e.g., Atmospheric Evaporative Demand (AED)), which may have a strong influence on drought severity, as evidenced in many hydrological (Vicente-Serrano et al., 2014) and ecological (Allen et al., 2015; Adams et al., 2017) applications. To overcome this we have also included in our analysis another popular drought index, the Standardized Precipitation Evapotranspiration Index (SPEI). Unlike the SPI, the SPEI accounts for both Precipitation (P) and Reference Evapotranspiration (ETo) as a representative metric to quantify the AED. The SPEI is based on a monthly climatic water balance (P-ETo), and is equally sensitive to variations in these two input variables (Vicente-Serrano et al., 2015). The P-ETo series of anomalies are adjusted using a three-parameter log–logistic distribution. The anomalies are accumulated at different time-scales, following the same approach used in the SPI, and converted to standard deviations with respect to average value (z-scores). Details on the calculation procedure of the SPEI can be found in Vicente-Serrano et al. (2010) and Beguería et al. (2014). The ETo was computed from air temperature data using the Hargreaves-Samani method (Hargreaves and Samani, 1985) as explained in the Section 2.1.2.

2.2.3. Statistical analysis

To quantify drought severity for each watershed and the sensitivity of streamflows to anomalies in each month of the year, we calculated the SPI and SPEI at time-scales varying from 1 to 48 months for each month of the year using the corresponding spatially-averaged series of P and ETo. For each watershed we obtained 576 series (12 months × 48

time-scales) for each drought index. Then, to account for the links between climatic droughts and hydrological droughts, we used the Pearson correlation coefficient, computed between the time series of SPEI/SPI for each time-scale and month of the year. All calculations were made for the entire study period (1940–2013), as well as for some selected sub-periods: 1940–1964, 1965–1989 and 1990–2013 to evaluate the stationarity of this correlation.

To summarize the high spatial variability exhibited by the relationship between SSI and SPEI/SPI, we performed a Principal Component Analysis (PCA) in S mode (Richman, 1986). In this mode, the data (i.e. correlations between SPEI/SPI and SSI in each basin) were structured in a matrix with 12 (months) rows by 48 (time-scales) columns per site, which represent the SPI-SSI or SPEI-SSI correlation structure in a month-time scale space. PCA analysis decomposes this month-time scale correlation space into a series of modes that represent independent amounts of the complexity (variance) in the SPI-SSI and/or SPEI-SSI correlation space.

The PCA procedure allows for the classification of 289 basins on the basis of the similarities of the principal components of the correlations between the SPEI/SPI and the SSI, and permits us to identify general patterns in these correlations. The number of the retained components was defined based on the percentage of the variance of the original month-time series correlation space explained by each component according to a scree-plot. We also mapped the PCA loadings for each watershed, which in our case is equivalent to the square root of the variance of the original space retained by each component, and identifies how much each principal component relates to the SPI/SPEI-SSI relationship of each watershed. We also classified the watersheds according to the maximum loading rule, in which each watershed was assigned to the PC that showed the highest loading. This analysis was conducted for the three selected sub-periods of the data record to analyze stationarity.

We also integrated information on soil, climate, topography and NDVI variables (see Section 2.1) in each watershed and analyzed how well they explain the spatial distribution of the loading patterns. This was done by spatially averaging and plotting the values of these biophysical variables and the PC Groups obtained from the maximum loading rule by means of boxplots for the entire period 1940–2013 as well as the three selected sub-periods.

Finally, to quantify the relative contribution of each of the biophysical variables explaining the spatial differences in SSI response to the SPEI at different time-scales, we applied a predictive discriminant analysis (PDA). The PDA explains the value of a dependent categorical variable based on its relationship to one or more predictors (Huberty, 1994). Given the presence of different independent variables, the PDA identifies the possible linear combinations of those predictors that best separate the groups of cases of the predicted; these combinations are termed discriminant functions (Hair et al., 1998). The PDA allowed identifying which predictors contributed more to the inter-category differences of the PC modes that summarize SSI–SPEI dependency.

3. Results

3.1. General patterns of response (1940–2013)

Fig. 2 shows the spatial distribution of the maximum correlation of the series of timescales between SPEI and SSI for each month and for the series of all months. Results are presented for the entire study period (1940–2013) and irrespective of any climatic and hydrological seasonal variations. Overall, Fig. 2 reveals high positive correlations in the majority of the analyzed basins, with only a few exceptions. One example of such an exception is the lower correlation found between SPEI and SSI along the Rocky Mountains and in the northeastern U.S. for the period February to April. These spatial patterns are very similar to the correlations between the SPEI and SSI (Supplementary Fig. 1). In both cases, there is clear dominance of positive and high correlations between SSI and SPEI during the different months of the year (Supplementary Fig. 2).

In general, maximum correlations between SPEI and SSI tend to be achieved at shorter time-scales, with averages ranging between 2- and 3-month SPEI (Supplementary Fig. 3), however, there are some regions that present maximum correlations at longer time scales. Notably, the snow regulated basins, particularly those in the western portions of the country, respond to longer SPEI time-scales than other basins. This pattern is evident for all months of the year and for the series of all months. This suggests differences in how these watersheds mediate the response of streamflow to climatic droughts (see Fig. 3).

The Principal Component Analysis confirms the existence of substantial variability in the patterns of hydrological droughts response. Specifically, it takes seven principal components to account for more than 80% of the total explained variance (Supplementary Fig. 4), each representing different spatial patterns of the month and time scale correlation between the SPEI and SSI.

Figs. 4 and 5 show the principal components and the principal component loadings, respectively. These figures identify the main hydrological drought response patterns to the range of climatic drought time-scales used in this analysis. The figures show substantial variations in the response of the analyzed basins, with coherent geographical patterns. In general, the PCs indicate a dominance of response to short SPEI time-scales, which is clearly represented in the first two components (Fig. 4). These two PCs explain 55% of the total variance. The loadings of PC1 show that this PC is representative of watersheds in the Southeast and the Midwest U.S. (Fig. 5). The mode of variation for PC1 (Fig. 4) show high correlations at SPEI time-scales lower than 10 months (Fig. 4), while the loadings of PC 2 show that this mode represents northeastern basins (Fig. 5), which show the strongest response at very short SPEI time-scales (less than 3 months) between April and January (Fig. 4). PC3 is representative of SPEI-SSI correlations in the US Pacific northwest region, with the highest correlation found at short SPEI time-scales between September and February. Significant correlations are also found between May and August, but only for longer SPEI time-scales. The loadings of PC 4 represents the SPEI-SSI relationship in the watersheds located in the Rocky Mountains, and the PC scores indicate that these basins are most responsive to climatic anomalies occurring between June and February at time-scales ranging from 8 to 18 months. The remaining PCs (PCs 5–7) represent local patterns, and small clusters of basins.

The PC analysis showing the spatial patterns of the SPI-SSI correlations are presented in Supplementary Figs. 5 through 7. These results show that the spatial modes of variation are similar to those analyzed using the SPEI and increases our confidence that the response of hydrological drought to climatic drought time-scales shows consistent spatial patterns, irrespective of the selected drought index.

3.2. Factors explaining the general response of SSI to SPEI time-scales

Fig. 6 shows the average values of the different topographic and environmental variables as a function of the PCs that summarize correlation patterns between SPEI and SSI. Annual average NDVI presents strong differences between PCs, with PCs 1, 2, 6 and 7 correlating with higher average NDVI than PCs 3, 4 and 5. Notably, PCs 3 and 6 show high intra-basin variability. Also, soil characteristics vary significantly between PCs, especially those related to water field capacity and depth of soil layer (the highest being recorded for PC 1). In contrast, soil drainage, infiltration and soil permeability do not present substantial differences between the different PCs. Similarly, basin area does not differ significantly between PCs. Average annual streamflow shows higher values for PCs 7 and 3, with high intra-basin variability among the basins belonging to these components. Average basin elevation presents noticeable differences between the PCs, with PCs 3 and 4 associated with higher elevations than the remaining components. Similarly, the PCs seem to vary with average annual minimum, maximum

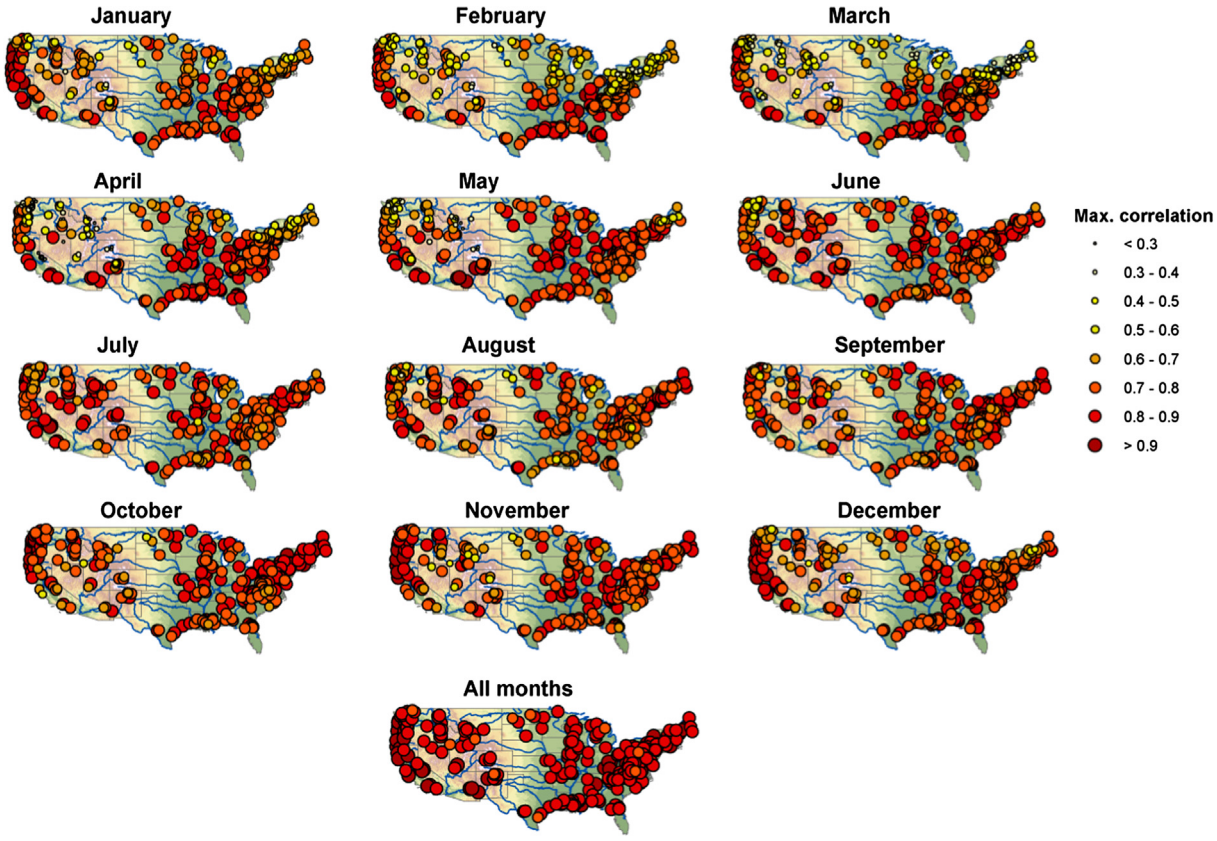

Fig. 2. Spatial distribution of maximum correlation between SPEI time-scales and SSI for each month independently and also for the series of all months.

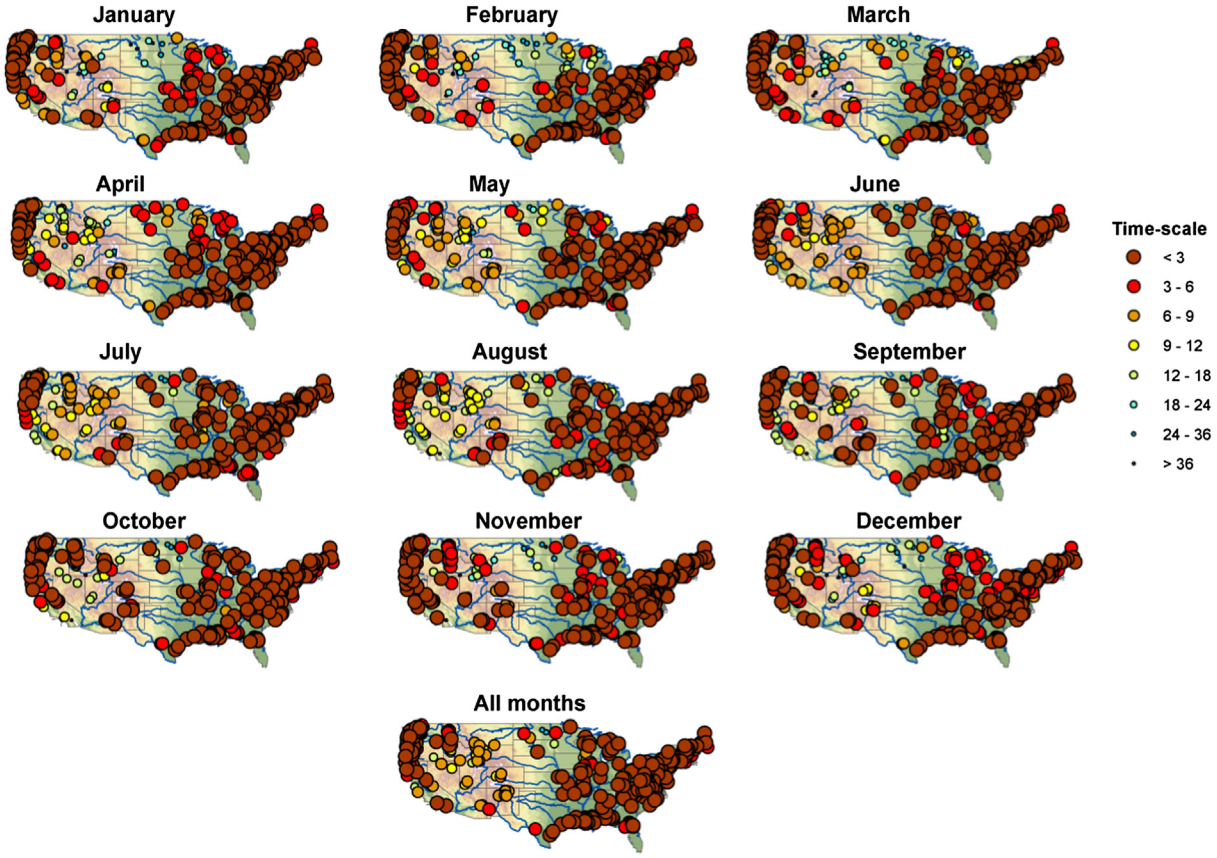

Fig. 3. Spatial distribution of the SPEI time-scale at which maximum correlation between SPEI time-scales and SSI is found for each month independently and also for the series of all months).

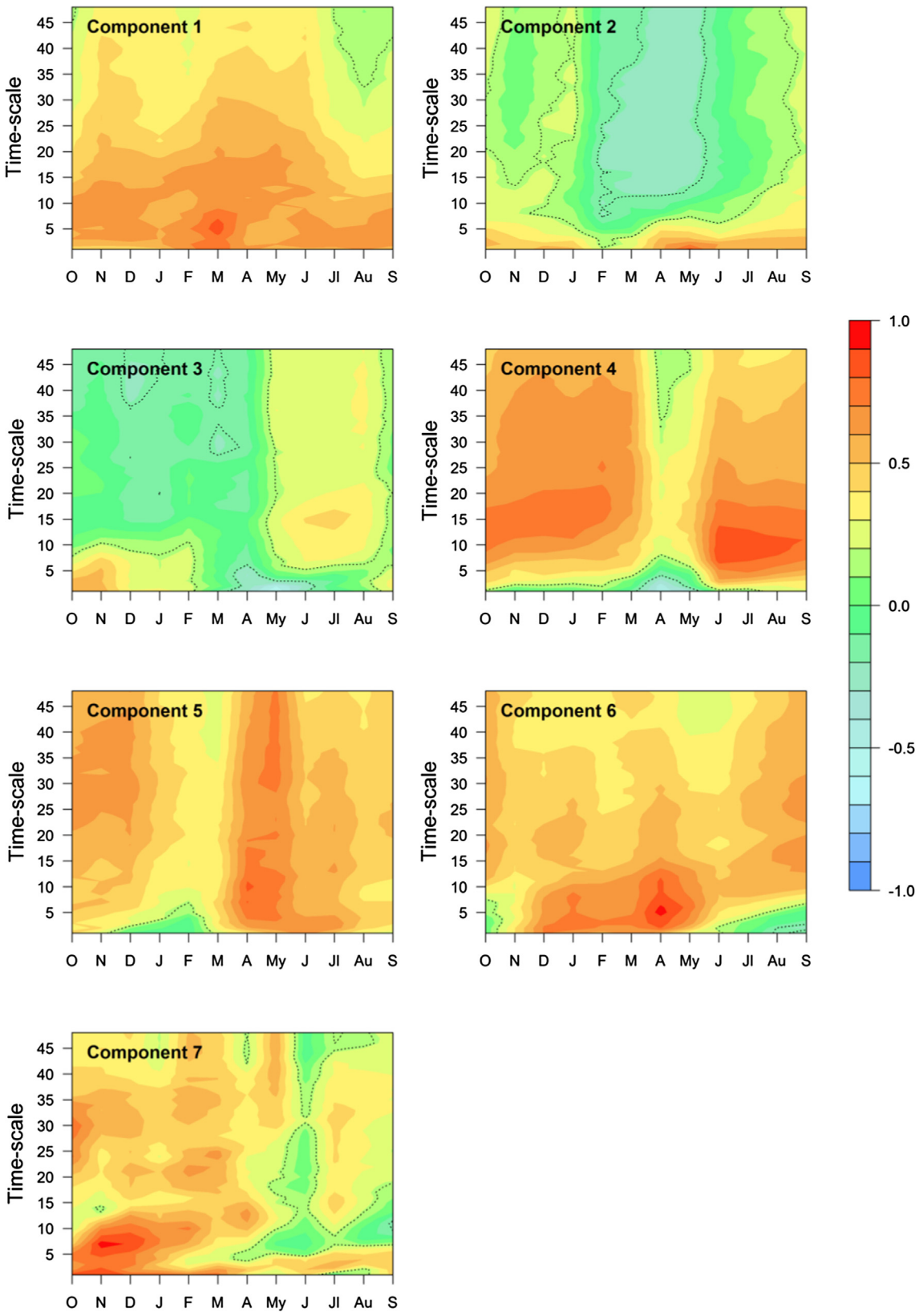

Fig. 4. Principal component scores obtained from correlations between SPEI time-scales and SSI (1940–2013). Dotted lines indicate significant correlations at $p < 0.05$.

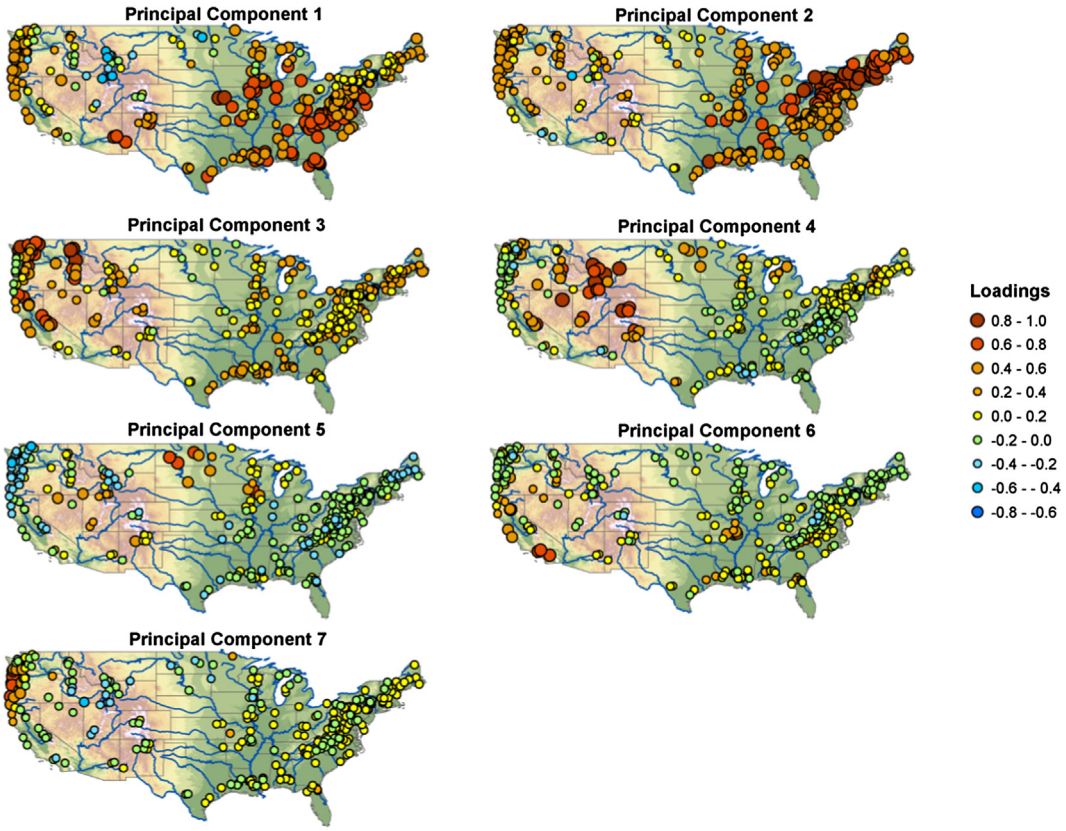

Fig. 5. Spatial distribution of the loadings of the extracted PCs, which summarize the patterns of correlation between SPEI time-scales and SSI.

temperature and ETo. PCs 3, 4 and 5 are characterized by lower temperatures than other components.

Table 1 shows the structure matrix following the results of the Predictive Discriminant Analysis (PDA), with three functions representing 43.8%, 27.7% and 10.5% of the total variance, respectively. Table 2 shows the centroids of the different components for the three predictive discriminant functions (PDFs). PC 1 and PC 2 show negative values for PDF 1, which has the greatest power to discriminate between the different independent variables. On the other hand, PCs 3, 4, 6 and 7 show positive values in PDF 1, indicating that the pattern of relationship between climatic and hydrologic droughts characteristics of PCs 1 and 2 is favored in areas with high vegetation coverage (NDVI). This feature is particularly evident during the warm season, when vegetation is more active. Positive values in PDF 1 are also associated with low elevations, high temperatures during the warm season, high precipitation during the warm season and low precipitation during the cold season. The patterns of relationship summarized by PCs 3 and 4, and to less extent PCs 6 and 7, are dominant in basins with opposite characteristics (i.e. low NDVI, high elevation, low temperatures and low precipitation during the warm season and high precipitation during the cold season). PDF 2 mostly discriminates between PCs 4 and 5 on the one hand and PC 7 on the other hand, demonstrating that PCs 4 and 5 are dominant in basins with low vegetation coverage, high elevation and low precipitation, while PC7 characterize watershed with high vegetation coverage in low elevation areas with relatively high precipitation. PDF 3 had low discrimination capacity and low values for the different variables. PDA also indicated that soil characteristics, average streamflow magnitude, and total surface area of the basins contributed less to discriminating between the different patterns of response of SSI to SPEI time-scales.

3.3. Temporal differences in the response of SSI to SPEI time-scales

The analysis applied for the different sub-periods (1940–1964, 1964–1989 and 1990–2013) reveal some differences in the relationship between climatic drought and hydrologic response in the U.S. The monthly correlation patterns in the month-time scale space between SSI and the SPEI shows that the general patterns for the entire period (1940–2013) are not exactly stationary in time. Between 1940 and 1964, the percentage of the variance absorbed by the first few PCs is similar to the variance absorbed by the PCs in the analysis of the entire period (Fig. 7). However, the subperiod 1965–1989 distributes the total variance between the PCs more evenly, and during the 1990–2013 period PC1 clearly represents a higher percentage of the total variance (Supplementary Fig. 8). The first two components of the 1940–1964 period maintain the response of SSI to SPEI at short time-scales, but with clear monthly differences (Fig. 7). The remaining components present a SSI response to longer SPEI time-scales, also with strong monthly differences. Nonetheless, these patterns have less spatial coherence, compared to those defined for the entire period (Supplementary Fig. 9).

The dominant patterns during 1965–1989 show some differences from those of the earlier period (Fig. 8). PC 1 shows higher correlations from medium to long time-scales between February and June and between July and November, while PC 2 exhibits significant correlations considering short SPEI time-scales between October and February. Similarly, PC 3 shows significant correlations at very short time-scales (1–2 months) between May and July. PC 4 presents a similar pattern than the same component calculated for the entire period, with significant correlations at longer time-scales, with the exception of April. These components show more coherent spatial patterns and are representative of larger regions than those of the earlier period (Supplementary Fig. 10). Compared to 1940–1964 and 1965–1989, the PCs in the analysis of the 1990–2013 period shows more granularity

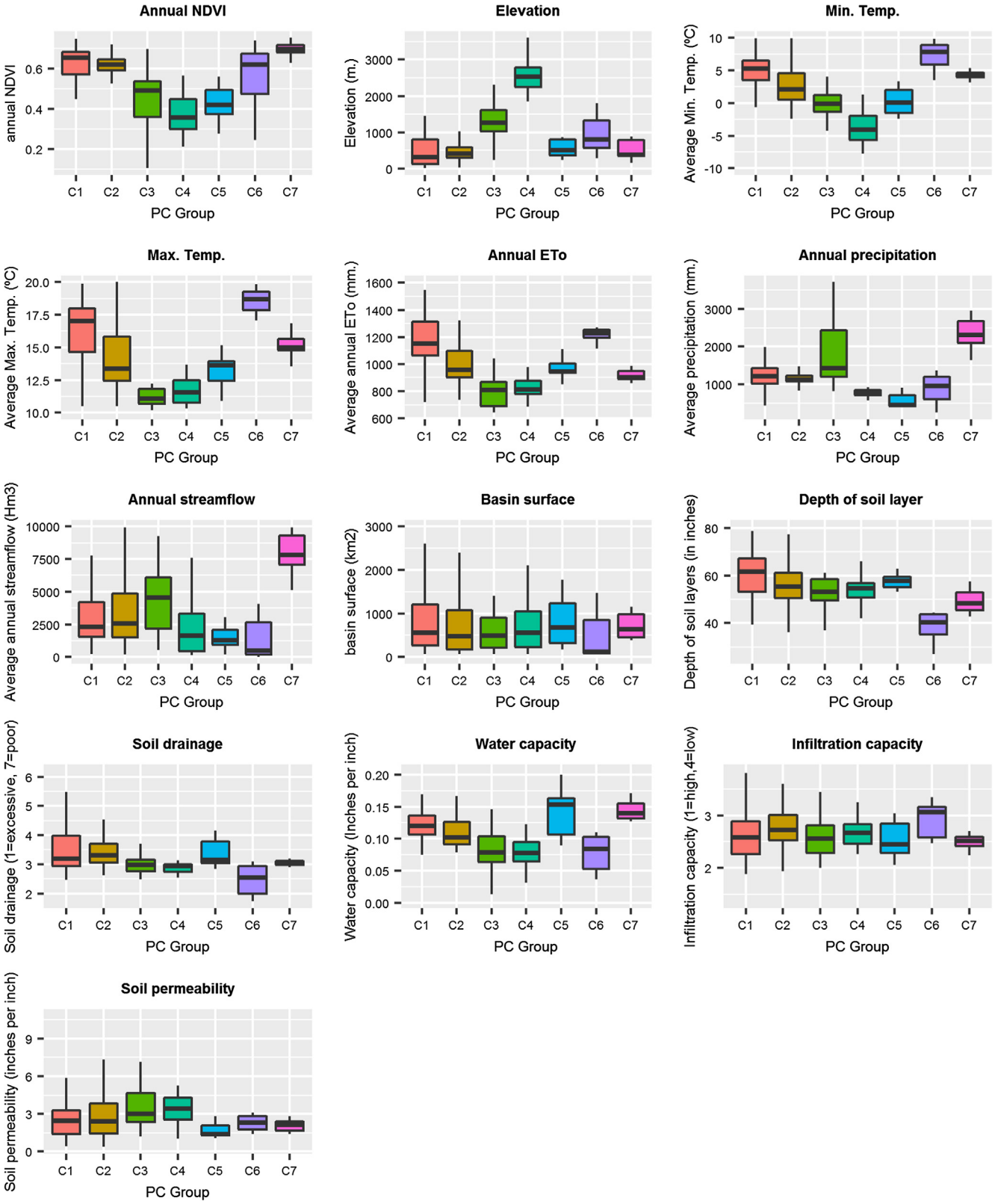

Fig. 6. Box-plots showing the average values of the different topographic and environmental variables corresponding to the seven retained PCs, which summarize the patterns of correlation between SSI and SPEI time-scales.

and variation (Fig. 9). The correlation patterns show distinct monthly responses to the range of SPEI time-scales, with smoother and more coherent spatial patterns. We noted PCs that represents the basins located in the northeastern (PC 1), southeastern U.S. (PC 2) and the Rocky Mountains (PC 5) (Supplementary Fig. 11). Overall, the spatial patterns of PC loadings and the analyzed response of the basins was very similar in the analysis done with any of the two drought indices -i.e. SPI and SPEI (Supplementary Figs. 12–18). This may indicate that

Table 1
Structure matrix of the PDA. Significant values ($p < 0.05$) are marked in bold.

	Function 1 (43.8%)	Function 2 (27.7%)	Function 3 (10.5%)
NDVI (annual)	**−0.459**	**0.551**	0.035
NDVI (cold season)	−0.365	**0.504**	0.11
NDVI (warm season)	**−0.515**	**0.545**	−0.053
Elevation	**0.488**	**−0.458**	−0.019
Min. Temperature (cold season)	−0.121	0.376	0.245
Min. Temperature (warm season)	**−0.45**	0.189	0.215
Min. Temperature (annual)	−0.286	0.299	0.24
Max. Temperature (annual)	−0.296	0.185	0.3
Max. Temperature (cold season)	−0.193	0.219	0.284
Max. Temperature (warm season)	−0.414	0.127	0.301
Eto (annual)	−0.303	0.073	0.298
Eto (cold season)	−0.223	0.078	0.237
Eto (warm season)	−0.358	0.064	0.337
Precipitation (annual)	0.199	**0.584**	−0.071
Precipitation (cold season)	0.431	**0.621**	−0.012
Precipitation (warm season)	−0.444	0.226	−0.179
Streamflow (annual)	0.137	0.222	−0.001
Streamflow (cold season)	0.09	0.402	0.16
Streamflow (warm season)	0.155	0.016	−0.147
Surface area	0.009	−0.155	0.277
Soil depth layer	−0.172	−0.041	0.065
Soil drainage	−0.213	0.038	−0.008
Soil water capacity	−0.259	0.179	0.478
Soil infiltration capacity	−0.022	−0.011	−0.126
Soil Permeability	0.094	−0.068	−0.169

Table 2
Centroids for the different components for the three discriminant functions.

Principal components	PDF 1	PDF 2	PDF 3
1	−0.857	0.014	0.503
2	−1,243	0.275	−0.703
3	3,557	0.523	−0.914
4	2,080	−2,571	0.15
5	−0.475	−2,319	2,282
6	2,002	0.313	0.626
7	2,252	4,888	1,917

the role of variations in the climatological water balance (P-ETo) is of secondary importance on the development of hydrological drought in the selected basins compared to variations in precipitation, which is the common input variable in the calculation of both SPI and SPEI. Our comparison also indicates that there is a general agreement on the magnitude of the maximum correlations found for the different sub-periods (Supplementary Figs. 19 and 20). However, and despite the overall agreement, there are some differences in terms of the SPEI time-scales at which the maximum correlations are recorded (Supplementary Figs. 21 and 22).

For the sub-periods 1940–1964 and 1965–1989, there are clear differences in the maximum correlation patterns found between SPEI and SSI (Supplementary Fig. 23). One representative example is the Rocky Mountains, where correlations increased from January to March, while decreased in April. In December, the magnitude of correlations clearly increased over the basins located in eastern and western portions of the country. On the other hand, while there are differences in the magnitude of maximum correlation patterns between the 1965–1989 and 1990–2013 periods (see for example, northern basins in January and February and western basins in April), their spatial patterns are more random than those found in the previous period (Supplementary Fig. 24). Notably, SPEI time-scales of maximum correlation are very different between sub-periods for some basins. In some cases, maximum correlations were found at longer SPEI time scales in one period, but at short time scales in the other (Supplementary Figs. 25 and 26). These findings indicate that the mechanisms that connect climatic and hydrological droughts may interact and reinforce or cancel each other out between the two periods. These mechanisms and their interactions are difficult to identify and evaluate because the small number of instances when maximum correlations shifted differently between SPEI time-scales in two periods makes comparisons with environmental and climatic variables (Supplementary Tables 1–4). Positive differences in maximum correlations between 1940 and 1964 and 1965–1989 (i.e. correlation of second period minus correlation of first period) are preferentially recorded for basins characterized by low NDVI values, high elevations, low ETo and temperature, but with clearly higher temperatures during the second period (Supplementary Table 1). This analysis seems to indicate that correlation differences between these two periods follow a spatial pattern related to the spatial distribution of these climatic and physiographical variables. However, the spatial patterns of differences in the SPEI time-scales at which maximum correlation is obtained between the two sub-periods do not show clear relationship with any of the analyzed climatologic or physiographical variables, with the exception of some monthly significant correlations (Supplementary Table 2).

The same analysis for sub-periods 1965–1989 and 1990–2013 show that the spatial patterns of maximum correlation difference may be controlled by the spatial patterns of precipitation, and mostly by the observed change in precipitation between the two sub-periods. Specifically, higher correlations during the second period tend to be primarily recorded for basins with low average precipitation, which makes an increase in annual and seasonal precipitation during the second sub-period more likely (Supplementary Table 3). Finally, differences in the time-scales at which the maximum correlation was recorded between these two periods did not reveal spatial patterns that correlate with the environmental and climatic variables analyzed here.

4. Discussion

In this study, we analyzed the response of a hydrological drought index (the Standardized Streamflow Index, SSI) to different time-scales of the Standardized Precipitation Evapotranspiration Index (SPEI) in different low anthropogenic perturbation watersheds across the U.S. Our findings indicate high correlations between the SPEI and SSI during a range of months of the year, confirming that the magnitude of hydrological droughts in the conterminous U.S. is strongly controlled by climatic droughts. The correlations found in this study are stronger than those obtained for basins impacted by water regulation and human management (e.g. Lorenzo-Lacruz et al., 2013; Vicente-Serrano et al., 2017b; Wu et al., 2017). With the exception of the February and April period, when correlations are generally lower, average correlations were around 0.8 or higher. For the all-months series, the average correlation was 0.9. These results highlight that hydrological droughts in natural basins are more influenced by climatic drought than in highly regulated basins, in which the temporal variability of hydrological droughts is controlled by other non-climatic factors, such as water storage capacity (Lorenzo-Lacruz et al., 2013) and dam operation rules (López-Moreno et al., 2009). Furthermore, water extraction and reallocation for different uses can also disrupt the relationship between climate variability and hydrological droughts (Tijdeman et al., 2018). However, the U.S. basins included in the analysis are considered to be relatively unperturbed by direct human action. Nevertheless, in some cases they can be affected by change in vegetation cover (e.g. recovery from past forest fires, ecological transitions), which can also affect the relationship between climatic and hydrologic droughts (García-Ruiz et al., 2008). Nevertheless, these potential vegetation cover changes are expected to have a local impact and it is most likely that hydrological drought responses in the studied basins are mainly controlled by climate variability.

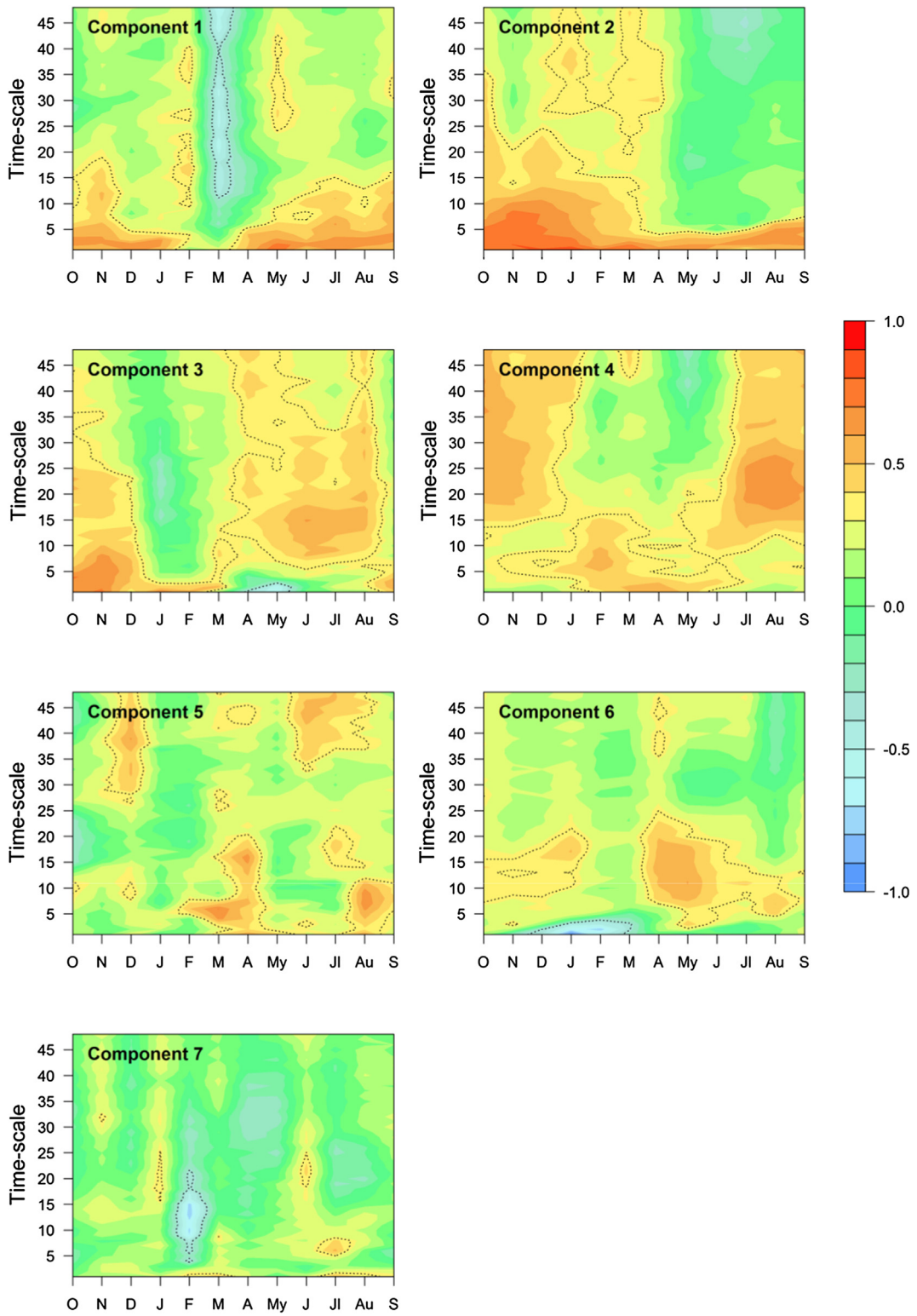

Fig. 7. Principal component scores obtained from monthly correlations between SPEI time-scales and SSI for the whole period 1940–1964. Dotted lines outline significant correlations at $p < 0.05$.

Another important finding is that SSI variability is mostly controlled by climatic droughts having characteristically short time-scales in the majority of the studied basins. Generally, our results show that the SPEI at time-scales between two and four months are often the most correlated with SSI. This clearly suggests that SSI in these natural basins responds to high frequency climate variability. Once again, these results are in contrast with results found in other studies for regulated basins (e.g. Lorenzo-Lacruz et al., 2010 and 2013), where variability of hydrological drought is mostly linked to climatic droughts of longer characteristic time scales and to streamflow drought conditions prolonged and exacerbated by water abstractions, transfers or impoundments (Tijdeman et al., 2018). These differences can reflect increased watershed storage, (e.g., reservoir storage), which modulates high frequency variations of upstream rain and streamflows, which induces

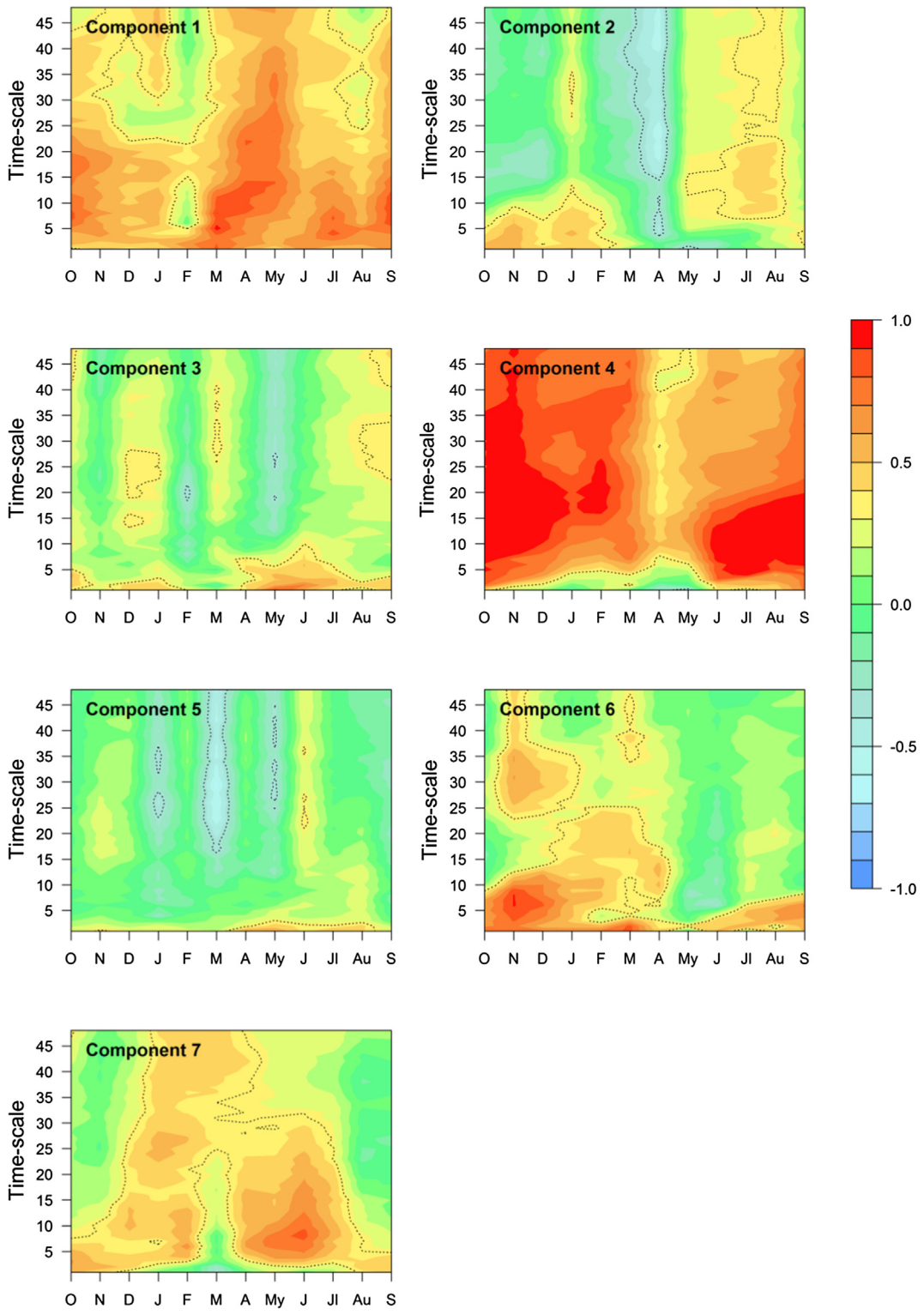

Fig. 8. Principal component scores obtained from the monthly correlations between SPEI time-scales and SSI for the sub-period 1965–1989. Dotted lines outline significant correlations at $p < 0.05$.

temporal autocorrelation and decreases the frequency of high peaks downstream (Lorenzo-Lacruz et al., 2010). In general, because of their higher capacity, hydrological drought conditions in reservoirs occur less frequently than in streamflows (Vicente-Serrano and López-Moreno, 2005; Wu et al., 2017) and even less frequently in groundwater systems (Bloomfield et al., 2015; Lorenzo-Lacruz et al., 2017). Our results align with the expectation that hydrologic drought response of the natural basins used in this study is mostly controlled by climatic drought.

We did, however, find some exceptions to the pattern of generally short timescales between meteorological and hydrological droughts. Some watersheds, mostly located in the Rocky Mountains, showed low correlations between the SPEI and SSI during the summer and winter months at shorter time scales, and appeared more responsive to long-

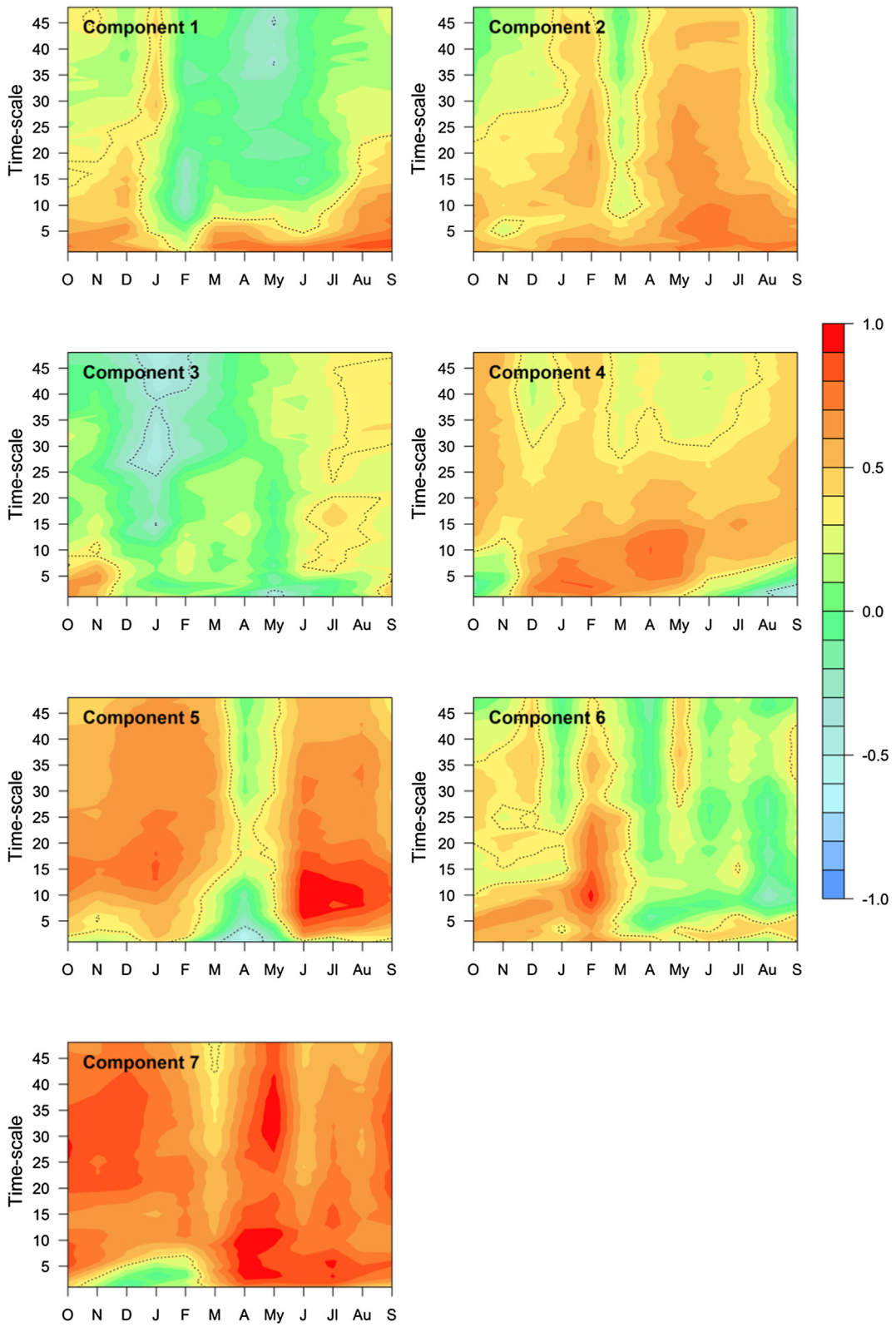

Fig. 9. Principal component scores obtained from correlations between SPEI time-scales and SSI for the sub-period 1990–2013. Dotted lines outline significant correlations at $p < 0.05$.

term SPEI time-scales during the spring and fall. This may be explained by the specific characteristics of the rivers located in this region, with streamflow driven by snow accumulation and melting, which are strongly controlled by temperature variability, instead of being directly controlled by rainfall variability. This was also found by Haslinger et al. (2014) and Rimkus et al. (2013), who found strong connections between hydrological and climatic droughts in Austria and Lithuania, except for those basins and seasons in which snow processes are important.

To ensure the results are robust and consistent, we conducted the

analysis with two widely used drought indices, the SPI (based only on precipitation data) and the SPEI (calculated using both precipitation and atmospheric evaporative demand). Vicente-Serrano et al. (2012) analyzed the relationship between streamflow variability and different drought indices in different basins worldwide. They reported that a higher correlation between climatic and streamflow anomalies was obtained when the SPEI was used instead of the SPI. However, increased AED also affects streamflow drought severity (e.g. Cai and Cowan, 2008; Cho et al., 2011; Teuling et al., 2013; Vicente-Serrano et al., 2017a). In this study there were negligible differences not only in the magnitude of correlations found between the SPI or the SPEI and the SSI, but also in the time scales and the seasonal patterns of these correlations. This finding suggests that in natural hydrological basins precipitation would have the greater influence on streamflow drought severity. Vicente-Serrano et al. (2014) showed that SSI in the Iberian Peninsula rivers responded better to SPEI than to SPI, especially in the summer months when the role of the AED is higher. However, they also reported that correlations between SPEI and SSI and SPI and SSI were similar for watersheds located in the headwaters where human intervention is more restricted and the effects of AED is lower. As the rivers reach their medium and low courses, temporal variability of streamflows is affected by AED, especially in the most regulated basins, where there is high surface coverage by irrigated lands (Vicente-Serrano et al., 2017b). In these circumstances, the SPEI explained streamflow anomalies better than the SPI.

Although we do not expect that the hydrological drought response patterns of the undisturbed watersheds analyzed in this study have the same degree of complexity than the regulated basins, we found remarkable spatial variations. This heterogeneity in the response of natural basins was also found by Barker et al. (2016) in > 120 catchments across the UK.

With a few exceptions, U.S. watersheds dominantly respond to climatic drought of short characteristic time-scales, but there were clear seasonal differences that confound homogeneous patterns in the correlations between SSI and climatic drought time-scales. Differences in the month-time scale correlation space of the different watersheds are mainly associated to differences in temperature, vegetation cover/use, as well as by topography (elevation).

Physiographic characteristics and vegetation coverage vary significantly from one river basin to another. In this analysis, we are considering a wide heterogeneous scenario to assess the response of hydrological drought to the climatic drought in a very diverse number of basins.

At this respect, we found out, as well as other studies related to this topic (Haslinger et al., 2014; Van Loon and Laaha, 2015), that not only precipitation but also elevation is one of the natural drivers that control the seasonality of the streamflows as AED directly depends on it (e.g. snow melt contribution to streamflows) and hence, the response of SSI to SPEI time-scales.

Regarding to the land use, vegetation has a major role as soil structure is directly related to the hydrological cycle processes (e.g. the runoff occurred during a heavy precipitation event or the water drainage from the aquifers to the watersheds). In addition, natural vegetation consumes water for respiration processes, being this the main disturbing factor that explains climate vs. streamflow relationships. This topic has been widely studied in the scientific literature (e.g. Bosch and Hewlett, 1982; de Jong et al., 2009; García-Ruiz et al., 2011; Llorens and Domingo, 2007)

The magnitude of streamflow, precipitation, soil characteristics and basin area also bring secondary contributions to these differences. The muted contribution of average annual and seasonal precipitation to explaining patterns of response of hydrologic drought contrasts with the findings of Tijdeman et al. (2016), who concluded that the characteristics and duration of hydrological drought in natural basins of the U.S. is mostly controlled by the precipitation characteristics of each basin.

This study also suggests that the mechanisms that propagate climatic droughts to streamflows may not be time stationary. This suggestion is based on the differences we have found in the magnitude of correlations and the time scales of maximum correlation between different periods in the record. The factors that drive this behavior are unclear, but they could be related to the non-linearity in the dynamics of watersheds during wet and dry periods, which affect how meteorological droughts propagate to become hydrological droughts (Haslinger et al., 2014). During the mega drought recorded in southeastern Australia in the 2000s, Yang et al. (2017) showed that the rainfall-runoff relationship was non-stationary, and that there were feedback mechanisms such that the duration and intensity of meteorological droughts were lengthened and amplified by the hydrological drought it generated. Non-stationarity driven by drought severity and catchment/land feedbacks adds some uncertainty to how climatological droughts propagate throughout the hydrological cycle. None of the explanatory variables used obtain insight into the spatial patterns of hydrologic drought were able to explain adequately why the magnitude of the differences and time-scales of maximum correlation was not stable between the analyzed sub-periods. The lack of explanatory power of the variables used in this study aligns with the results presented by Yang et al. (2017), who found that the times of recovery of hydrological drought conditions in relation to climatic droughts are not related to the catchment landscape. They confirmed that the impact of other hydro-climatic factors and catchment properties is minimal.

Recent studies have suggested the use of climatic information to predict hydrological droughts (e.g. Zhu et al., 2016; Yuan, et al., 2017), which is especially appealing to characterize hydrological drought in regions where streamflow data is not available. However, results from this study, and specifically the evidence of non-stationary mechanisms in the response of hydrological droughts to climate variability, suggest that making robust predictions using only climatological information will be a challenging task, even in natural basins, where most of streamflow behavior is expected to respond to climate variability. The complexity of physiographic, climatic, edaphic and mostly vegetation characteristics drive a complex and non-stationary behavior, which is very difficult to determine.

In summary, we have showed that the response of hydrological droughts to climatic droughts is complex, especially in terms of the climatic drought time-scales that are more likely to control hydrological drought severity. This is expected in strongly modified and regulated basins, where water management and/or dam operation rules may strongly alter this behavior. In this study it has been demonstrated that the response of hydrological droughts to climatic drought conditions can be complex and non-stationary, even in natural basins. Within the conterminous U.S. very different patterns of hydrological drought responses to climatic drought time-scales have been detected. These natural basins are characterized by different climatological, physiographical and vegetation conditions. Further research is necessary to understand the role of vegetation cover change on the non-stationary behavior of hydrological drought response detected in this study, and to define to what extent the connection between climatic and hydrologic drought is disrupted by different levels of human management and practices in the United States.

5. Conclusions

In conclusion, we summarize the main findings of this study:

- The magnitude of hydrological droughts in U.S. depends directly on climatic droughts, and this relationship is stronger in natural basins than in regulated basins.
- In natural basins, the SSI responds predominantly to high frequency climate variability.
- The time scales and seasonal response of SSI to SPEI and SPI suggest that hydrological basins precipitation would have the greatest

influence on streamflow drought severity.

- However, in the contiguous U.S., a noteworthy spatial variation and heterogeneity in the response of natural basins exist. In mountainous river basins, hydrological droughts were found exceptionally to be controlled not only by precipitation variability but also by temperature at long-term.
- At this respect, not only climatic conditions influence hydrological droughts. Soil characteristics, vegetation or physical characteristics of the basins also determine the different patterns of response found in natural regimes.

Acknowledgements

This work was supported by the research project I-Link1001 (Validation of climate drought indices for multi-sectorial applications in North America and Europe under a global warming scenario) financed by CSIC, PCIN-2015-220 and CGL2014-52135-C03-01 financed by the Spanish Commission of Science and Technology and FEDER, IMDROFLOOD financed by the Water Works 2014 co-funded call of the European Commission and INDECIS, which is part of ERA4CS, an ERA-NET initiated by JPI Climate, and funded by FORMAS (SE), DLR (DE), BMWFW (AT), IFD (DK), MINECO (ES), ANR (FR) with co-funding by the European Union (Grant 690462). Marina Peña-Gallardo was granted by the Spanish Ministry of Economy and Competitiveness. Miquel Tomas-Burguera was supported by a doctoral grant by the Spanish Ministry of Education, Culture and Sport. Jamie Hannaford was supported by the Belmont Forum project 'DrIVER', NERC Grant Number (grant NE/L010038/1). Marco Maneta acknowledges support from the USDA NIFA grant 2016-67026-25067.

Appendix A. Supplementary material

Supplementary data to this article can be found online at https://doi.org/10.1016/j.jhydrol.2018.11.026.

References

Adams, H.D., Zeppel, M.J.B., Anderegg, W.R.L., Hartmann, H., Landhäusser, S.M., Tissue, D.T., Huxman, T.E., Hudson, P.J., Franz, T.E., Allen, C.D., Anderegg, L.D.L., Barron-Gafford, G.A., Beerling, D.J., Breshears, D.D., Brodribb, T.J., Bugmann, H., Cobb, R.C., Collins, A.D., Dickman, L.T., Duan, H., Ewers, B.E., Galiano, L., Galvez, D.A., Garcia-Forner, N., Gaylord, M.L., Germino, M.J., Gessler, A., Hacke, U.G., Hakamada, R., Hector, A., Jenkins, M.W., Kane, J.M., Kolb, T.E., Law, D.J., Lewis, J.D., Limousin, J.-M., Love, D.M., Macalady, A.K., Martínez-Vilalta, J., Mencuccini, M., Mitchell, P.J., Muss, J.D., O'Brien, M.J., O'Grady, A.P., Pangle, R.E., Pinkard, E.A., Piper, F.I., Plaut, J.A., Pockman, W.T., Quirk, J., Reinhardt, K., Ripullone, F., Ryan, M.G., Sala, A., Sevanto, S., Sperry, J.S., Vargas, R., Vennetier, M., Way, D.A., Xu, C., Yepez, E.A., McDowell, N.G., 2017. A multi-species synthesis of physiological mechanisms in drought-induced tree mortality. Nat. Ecol. Evol. 1, 1285–1291. https://doi.org/10.1038/s41559-017-0248-x.

Allen, C.D., Breshears, D.D., McDowell, N.G., 2015. On underestimation of global vulnerability to tree mortality and forest die-off from hotter drought in the Anthropocene. Ecosphere 6, art129. https://doi.org/10.1890/ES15-00203.1.

Allen, R.G., 1998. Crop evapotranspiration: guidelines for computing crop water requirements. Food Agric. Org. United Nations.

Bąk, B., Kubiak-Wójcicka, K., 2017. Impact of meteorological drought on hydrological drought in Toruń (central Poland) in the period of 1971–2015. J. Water L. Dev. 32. https://doi.org/10.1515/jwld-2017-0001.

Bandaru, V., Pei, Y., Hart, Q., Jenkins, B.M., 2017. Impact of biases in gridded weather datasets on biomass estimates of short rotation woody cropping systems. Agric. For. Meteorol. 233, 71–79. https://doi.org/10.1016/J.AGRFORMET.2016.11.008.

Barker, L.J., Hannaford, J., Chiverton, A., Svensson, C., 2016. From meteorological to hydrological drought using standardised indicators. Hydrol. Earth Syst. Sci. 20, 2483–2505. https://doi.org/10.5194/hess-20-2483-2016.

Beguería, S., Vicente-Serrano, S.M., Reig, F., Latorre, B., 2014. Standardized precipitation evapotranspiration index (SPEI) revisited: parameter fitting, evapotranspiration models, tools, datasets and drought monitoring. Int. J. Climatol. 34, 3001–3023. https://doi.org/10.1002/joc.3887.

Bloomfield, J.P., Marchant, B.P., Bricker, S.H., Morgan, R.B., 2015. Regional analysis of groundwater droughts using hydrograph classification. Hydrol. Earth Syst. Sci. 19, 4327–4344. https://doi.org/10.5194/hess-19-4327-2015.

Bodner, G.S., Robles, M.D., 2017. Enduring a decade of drought: patterns and drivers of vegetation change in a semi-arid grassland. J. Arid Environ. 136, 1–14. https://doi.org/10.1016/J.JARIDENV.2016.09.002.

Bosch, J.M., Hewlett, J.D., 1982. A review of catchment experiments to determine the effect of vegetation changes on water yield and evapotranspiration. J. Hydrol. 55, 3–23. https://doi.org/10.1016/0022-1694(82)90117-2.

Cai, W., Cowan, T., 2008. Dynamics of late autumn rainfall reduction over southeastern Australia. Geophys. Res. Lett. 35, L09708. https://doi.org/10.1029/2008GL033727.

Carlson, T.N., Ripley, D.A., 1997. On the relation between NDVI, fractional vegetation cover, and leaf area index. Remote Sens. Environ. 62, 241–252. https://doi.org/10.1016/S0034-4257(97)00104-1.

Cho, J., Komatsu, H., Pokhrel, Y., Yeh, P.J.-F., Oki, T., Kanae, S., 2011. The effects of annual precipitation and mean air temperature on annual runoff in global forest regions. Clim. Change 108, 401–410. https://doi.org/10.1007/s10584-011-0197-3.

Daly, C., Halbleib, M., Smith, J.I., Gibson, W.P., Doggett, M.K., Taylor, G.H., Curtis, J., Pasteris, P.P., 2008. Physiographically sensitive mapping of climatological temperature and precipitation across the conterminous United States. Int. J. Climatol. 28, 2031–2064. https://doi.org/10.1002/joc.1688.

de Jong, C., Lawler, D., Essery, R., 2009. Mountain Hydroclimatology and Snow Seasonality- Perspectives on climate impacts, snow seasonality and hydrological change in mountain environments. Hydrol. Process. 23, 955–961. https://doi.org/10.1002/hyp.7193.

Fiorillo, F., Guadagno, F.M., 2010. Karst spring discharges analysis in relation to drought periods, using the SPI. Water Resour. Manage. 24, 1867–1884. https://doi.org/10.1007/s11269-009-9528-9.

García-Ruiz, J.M., Regüés, D., Alvera, B., Lana-Renault, N., Serrano-Muela, P., Nadal-Romero, E., Navas, A., Latron, J., Martí-Bono, C., Arnáez, J., 2008. Flood generation and sediment transport in experimental catchments affected by land use changes in the central Pyrenees. J. Hydrol. 356, 245–260. https://doi.org/10.1016/j.jhydrol.2008.04.013.

García-Ruiz, J.M., López-Moreno, J.I., Vicente-Serrano, S.M., Lasanta–Martínez, T., Beguería, S., 2011. Mediterranean water resources in a global change scenario. Earth-Science Rev. 105, 121–139. https://doi.org/10.1016/J.EARSCIREV.2011.01.006.

Hair, J.F., Black, W.C., Babin, B.J., Anderson, R.E., 1998. Multivariate Data Analysis. Prentice Hall, New York.

Hargreaves, G.H., Samani, Z.A., 1985. Reference crop evapotranspiration from temperature. Appl. Eng. Agric. 1, 96–99. https://doi.org/10.13031/2013.26773.

Haslinger, K., Koffler, D., Schöner, W., Laaha, G., 2014. Exploring the link between meteorological drought and streamflow: effects of climate-catchment interaction. Water Resour. Res. 50, 2468–2487. https://doi.org/10.1002/2013WR015051.

Heim, R.R., 2002. A Review of Twentieth-Century Drought Indices Used in the United States. Bull. Am. Meteorol. Soc. 83, 1149–1165. https://doi.org/10.1175/1520-0477(2002)083<1149:AROTDI>2.3.CO;2.

Hobbins, M.T., Wood, A., McEvoy, D.J., Huntington, J.L., Morton, C., Anderson, M., Hain, C., Hobbins, M.T., Wood, A., McEvoy, D.J., Huntington, J.L., Morton, C., Anderson, M., Hain, C., 2016. The Evaporative Demand Drought Index. Part I: Linking Drought Evolution to Variations in Evaporative Demand. J. Hydrometeorol. 17, 1745–1761. https://doi.org/10.1175/JHM-D-15-0121.1.

Huang, S., Li, P., Huang, Q., Leng, G., Hou, B., Ma, L., 2017. The propagation from meteorological to hydrological drought and its potential influence factors. J. Hydrol. 547, 184–195. https://doi.org/10.1016/J.JHYDROL.2017.01.041.

Huberty, C.J., 1994. Why multivariable analyses? Educ. Psychol. Meas. 54, 620–627. https://doi.org/10.1177/0013164494054003005.

Llorens, P., Domingo, F., 2007. Rainfall partitioning by vegetation under Mediterranean conditions. A review of studies in Europe. J. Hydrol. 335, 37–54. https://doi.org/10.1016/J.JHYDROL.2006.10.032.

López-Moreno, J.I., Vicente-Serrano, S.M., Beguería, S., García-Ruiz, J.M., Portela, M.M., Almeida, A.B., 2009. Dam effects on droughts magnitude and duration in a transboundary basin: The Lower River Tagus, Spain and Portugal. Water Resour. Res. 45. https://doi.org/10.1029/2008WR007198.

López-Moreno, J.I., Vicente-Serrano, S.M., Zabalza, J., Beguería, S., Lorenzo-Lacruz, J., Azorin-Molina, C., Morán-Tejeda, E., 2013. Hydrological response to climate variability at different time scales: a study in the Ebro basin. J. Hydrol. 477, 175–188. https://doi.org/10.1016/J.JHYDROL.2012.11.028.

Lorenzo-Lacruz, J., Garcia, C., Morán-Tejeda, E., 2017. Groundwater level responses to precipitation variability in Mediterranean insular aquifers. J. Hydrol. 552, 516–531. https://doi.org/10.1016/J.JHYDROL.2017.07.011.

Lorenzo-Lacruz, J., Vicente-Serrano, S., González-Hidalgo, J., López-Moreno, J., Cortesi, N., 2013. Hydrological drought response to meteorological drought in the Iberian Peninsula. Clim. Res. 58, 117–131. https://doi.org/10.3354/cr01177.

Lorenzo-Lacruz, J., Vicente-Serrano, S.M., López-Moreno, J.I., Beguería, S., García-Ruiz, J.M., Cuadrat, J.M., 2010. The impact of droughts and water management on various hydrological systems in the headwaters of the Tagus River (central Spain). J. Hydrol. 386, 13–26. https://doi.org/10.1016/j.jhydrol.2010.01.001.

Lutz, J.A., van Wagtendonk, J.W., Franklin, J.F., 2010. Climatic water deficit, tree species ranges, and climate change in Yosemite National Park. J. Biogeogr. 37, 936–950. https://doi.org/10.1111/j.1365-2699.2009.02268.x.

Mckee, T.B., Doesken, N.J., Kleist, J., 1993. The relationshio of drought frequency and duration to time scales. Eighth Conf. Appl. Climatol. 17–22.

Merheb, M., Moussa, R., Abdallah, C., Colin, F., Perrin, C., Baghdadi, N., 2016. Hydrological response characteristics of Mediterranean catchments at different time scales: a meta-analysis. Hydrol. Sci. J. 61, 2520–2539. https://doi.org/10.1080/02626667.2016.1140174.

Redmond, K.T., 2002. The depiction of drought. Bull. Am. Meteorol. Soc. 83, 1143–1148. https://doi.org/10.1175/1520-0477-83.8.1143.

Richman, M.B., 1986. Rotation of principal components. J. Climatol. 6, 293–335. https://doi.org/10.1002/joc.3370060305.

Rimkus, E., Stonevičius, E., Korneev, V., Kažys, J., Valiuškevičius, G., Pakhomau, A., 2013. Dynamics of meteorological and hydrological droughts in the Neman river

basin. Environ. Res. Lett. 8, 045014. https://doi.org/10.1088/1748-9326/8/4/045014.
Scaini, A., Sánchez, N., Vicente-Serrano, S.M., Martínez-Fernández, J., 2015. SMOS-derived soil moisture anomalies and drought indices: a comparative analysis using in situ measurements. Hydrol. Process. 29, 373–383. https://doi.org/10.1002/hyp.10150.
Sheffield, J., Wood, E.F., 2011. In: Sheffield, J., Wood, E.F. (Eds.), GNHRE. Earthscan, London and Washington DC.
State Soil Geographic (STATSG0), 1991. Data Base Data use information. Publication Number 1492. U.S. Department of Agriculture, Natural Resources Conservation Service. Fort Worth, Texas.
Tallaksen, L.M., Van Lanen, H.A., 2004. Hydrological drought : processes and estimation methods for streamflow and groundwater. Developments in Water Science, 48th ed. Elsevier Science B.V., Amsterdam, the Netherlands.
Tallaksen, L.M., Madsen, H., Hisdal, H., 2004. Frequency analysis. In: Tallaksen, L.M., van Lanen, H.A.J. (Eds.), Hydrological Drought Processes and Estimation Methods for Streamflow and Groundwater. Elsevier Science, Amsterdam, pp. 199–271.
Teuling, A.J., Van Loon, A.F., Seneviratne, S.I., Lehner, I., Aubinet, M., Heinesch, B., Bernhofer, C., Grünwald, T., Prasse, H., Spank, U., 2013. Evapotranspiration amplifies European summer drought. Geophys. Res. Lett. 40, 2071–2075. https://doi.org/10.1002/grl.50495.
Tijdeman, E., Bachmair, S., Stahl, K., 2016. Controls on hydrologic drought duration in near-natural streamflow in Europe and the USA. Hydrol. Earth Syst. Sci. 20, 4043–4059. https://doi.org/10.5194/hess-20-4043-2016.
Tijdeman, E., Hannaford, J., Stahl, K., 2018. Human influences on streamflow drought characteristics in England and Wales. Hydrol. Earth Syst. Sci. 22, 1051–1064. https://doi.org/10.5194/hess-22-1051-2018.
Van Loon, A.F., 2015. Hydrological drought explained. Wiley Interdiscip. Rev. Water 2, 359–392. https://doi.org/10.1002/wat2.1085.
Van Loon, A.F., Laaha, G., 2015. Hydrological drought severity explained by climate and catchment characteristics. J. Hydrol. 526, 3–14. https://doi.org/10.1016/J.JHYDROL.2014.10.059.
Vicente-Serrano, S.M, Miralles, Diego Gonzalez, Domínguez-Castro, Fernando, Azorin-Molina, Cesar, El Kenawy, Ahmed, McVicar, Tim R, Tomás-Burguera, Miquel, Beguería, Santiago, Maneta, Marco, Peña-Gallardo, Marina, 2018. Global Assessment of the Standardized Evapotranspiration Deficit Index (SEDI) for Drought Analysis and Monitoring. J.Climate 31 (14), 5371–5393.
Vicente-Serrano, S.M., Beguería, S., López-Moreno, J.I., 2011. Comment on "Characteristics and trends in various forms of the Palmer Drought Severity Index (PDSI) during 1900–2008" by Aiguo Dai. J. Geophys. Res. 116, D19112. https://doi.org/10.1029/2011JD016410.
Vicente-Serrano, S.M., Beguería, S., López-Moreno, J.I., Vicente-Serrano, S.M., Beguería, S., López-Moreno, J.I., 2010. A multiscalar drought index sensitive to global warming: the standardized precipitation evapotranspiration index. J. Clim. 23, 1696–1718. https://doi.org/10.1175/2009JCLI2909.1.
Vicente-Serrano, S.M., Lopez-Moreno, J.-I., Beguería, S., Lorenzo-Lacruz, J., Sanchez-Lorenzo, A., García-Ruiz, J.M., Azorin-Molina, C., Morán-Tejeda, E., Revuelto, J., Trigo, R., Coelho, F., Espejo, F., 2014. Evidence of increasing drought severity caused by temperature rise in southern Europe. Environ. Res. Lett. Environ. Res. Lett. 9, 44001–44009. https://doi.org/10.1088/1748-9326/9/4/044001.
Vicente-Serrano, S.M., López-Moreno, J.I., 2005. Hydrological response to different time scales of climatological drought: an evaluation of the Standardized Precipitation Index in a mountainous Mediterranean basin. Hydrol. Earth Syst. Sci. 9, 523–533. https://doi.org/10.5194/hess-9-523-2005.
Vicente-Serrano, S.M., López-Moreno, J.I., Beguería, S., Lorenzo-Lacruz, J., Azorin-Molina, C., Morán-Tejeda, E., 2012. Accurate computation of a streamflow drought index. J. Hydrol. Eng. 17, 318–332. https://doi.org/10.1061/(ASCE)HE.1943-5584.0000433.
Vicente-Serrano, S.M., Van der Schrier, G., Beguería, S., Azorin-Molina, C., Lopez-Moreno, J.-I., 2015. Contribution of precipitation and reference evapotranspiration to drought indices under different climates. J. Hydrol. 526, 42–54. https://doi.org/10.1016/j.jhydrol.2014.11.025.
Vicente-Serrano, S.M., Zabalza-Martínez, J., Borràs, G., López-Moreno, J.I., Pla, E., Pascual, D., Savé, R., Biel, C., Funes, I., Azorin-Molina, C., Sanchez-Lorenzo, A., Martín-Hernández, N., Peña-Gallardo, M., Alonso-González, E., Tomas-Burguera, M., El Kenawy, A., 2017a. Extreme hydrological events and the influence of reservoirs in a highly regulated river basin of northeastern Spain. J. Hydrol. Reg. Stud. 12, 13–32. https://doi.org/10.1016/j.ejrh.2017.01.004.
Vicente-Serrano, S.M., Zabalza-Martínez, J., Borràs, G., López-Moreno, J.I., Pla, E., Pascual, D., Savé, R., Biel, C., Funes, I., Martín-Hernández, N., Peña-Gallardo, M., Beguería, S., Tomas-Burguera, M., 2017b. Effect of reservoirs on streamflow and river regimes in a heavily regulated river basin of Northeast Spain. CATENA 149, 727–741. https://doi.org/10.1016/j.catena.2016.03.042.
WMO, 2012. Standardized Precipitation Index User Guide.
Wu, J., Chen, X., Yao, H., Gao, L., Chen, Y., Liu, M., 2017. Non-linear relationship of hydrological drought responding to meteorological drought and impact of a large reservoir. J. Hydrol. 551, 495–507. https://doi.org/10.1016/J.JHYDROL.2017.06.029.
Yang, Y., McVicar, T.R., Donohue, R.J., Zhang, Y., Roderick, M.L., Chiew, F.H.S., Zhang, L., Zhang, J., 2017. Lags in hydrologic recovery following an extreme drought: assessing the roles of climate and catchment characteristics. Water Resour. Res. 53, 4821–4837. https://doi.org/10.1002/2017WR020683.
Yuan, X., Zhang, M., Wang, L., Zhou, T., 2017. Understanding and seasonal forecasting of hydrological drought in the Anthropocene. Hydrol. Earth Syst. Sci. 21, 5477–5492. https://doi.org/10.5194/hess-21-5477-2017.
Zhu, Y., Wang, W., Singh, V.P., Liu, Y., 2016. Combined use of meteorological drought indices at multi-time scales for improving hydrological drought detection. Sci. Total Environ. 571, 1058–1068. https://doi.org/10.1016/J.SCITOTENV.2016.07.096.